# Lattice Independent Component Analysis for fMRI

Manuel Graña, Darya Chyzhyk, Maite García-Sebastián, Carmen Hernández

*Computational Intelligence Group*
*Dept. CCIA, UPV/EHU, Apdo. 649, 20080 San Sebastian, Spain*
*www.ehu.es/ccwintco*

**Abstract**

We introduce a Lattice Independent Component Analysis (LICA) approach to fMRI analysis based on an Incremental Lattice Source Induction Algorithm (ILSIA). The ILSIA is grounded in recent theoretical results on Lattice Associative Memories (LAM). It aims to select a set of Strong Lattice Independent (SLI) vectors from the input dataset. Those SLI vectors can be assumed to be an Affine Independent set of vectors which define a convex polytope on the input data space. We call them *lattice sources*. They are used to compute the linear unmixing of each voxel's time series independently. The resulting mixing coefficients roughly correspond to the Independent Component Analysis (ICA) mixing matrix, while the set of lattice sources corresponds to the statistically independent sources found by ICA. The proposed approach is unsupervised or model free because the design matrix containing the regressors is not fixed *a priori* but induced from the data. Our approach does not impose any probabilistic model on the searched sources, although we assume a linear mixture model. We show on simulated fMRI data that our approach can discover the meaningful sources with efficiency comparable to that of ICA. Besides, on a well-known case study our approach can discover activation patterns in good agreement with the state of the art Statistical Parametric Mapping (SPM) software, and some state of the art ICA variants.

*Key words:* Lattice Independence, Lattice Associative Memories, fMRI, Independent Component Analysis

## 1. Introduction

Human brain mapping is a rapidly expanding discipline, and in recent years interest has grown in novel methods for imaging human brain functionality. Noninvasive techniques can measure cerebral physiologic responses during neural activation. One of the relevant techniques is functional Magnetic Resonance Imaging (fMRI) [18], which uses the blood oxygenation level dependent (BOLD) contrast to detect physiological alterations, such as neuronal activation resulting in changes of blood flow and blood oxygenation. The signal changes are related to changes in the concentration of deoxyhemoglobin, which acts as an intravascular contrast agent for fMRI. Most of the fMRI examinations are performed using T2 weighted spin echo pulse sequences or T2* weighted gradient echo pulse sequences. The various fMRI-methods have a good

spatial and temporal resolution, limited only by the precision with which the autoregulatory mechanisms of the brain adjust blood flow in space to the metabolic demands of neuronal activity. Since these methods are completely noninvasive, using no contrast agent or ionizing radiation, repeated single-subject studies are becoming feasible [17].

An fMRI experiment consists of a functional template or protocol (e.g., alternating activation and rest for a certain time) that induces a functional response in the brain. The aim of the experiment is to detect the response to this time varying stimulus, through the examination of the signal resulting from the BOLD effect, in a defined volume element (voxel). The functional information of a voxel has to be extracted from its time series. One fMRI volume is recorded at each sampling time instant during the experiment. The time sampling frequency is determined by the resolution of the fMRI imaging pulse sequence. The complete four-dimensional dataset (three dimensions in space, one dimension in time) consists of subsequently recorded three-dimensional (3-D) volumes. The acquisition of these functional volumes runs over periods lasting up to several minutes.

The most extended analysis approach for fMRI signals is the Statistical Parametric Maps (SPM) [6, 5], which has evolved into a free software package. This method consists in the separate voxel estimation of the regression parameters of General Linear Model (GLM), whose design matrix has been built corresponding to the experimental design. A contrast is then defined on the estimated regression parameters, which can take the form of a t-test or an F-test. The theory of Random Fields is then applied to correct the test thresholds, taking into account the spatial correlation of the independent test results.

There have been also approaches to the fMRI analysis based on the Independent Component Analysis (ICA) [3] assuming that the time series observations are linear mixtures of independent sources which can not be observed. ICA assumes that the source signals are non-Gaussian and that the linear mixing process is unknown. The approaches to solve the ICA problem obtain both the independent sources and the linear unmixing matrix. These approaches are unsupervised because no *a priori* information about the sources or the mixing process is included, hence the alternative name of Blind Deconvolution.

In this paper we propose an approach that we call Lattice Independent Component Analysis (LICA) that consists of two steps. Firts it selects Strong Lattice Independent (SLI) vectors from the input dataset using an incremental algorithm, the Incremental Lattice Source Induction Algorithm (ILSIA). Second, because of the conjectured equivalence between SLI and Affine Independence, it performs the linear unmixing of the input dataset based on these lattice sources. Therefore, the approach is a mixture of linear and nonlinear methods.

The original works were devoted to unsupervised hyperspectral image segmentation, therefore the use of the term *endmembers* for the selected vectors in previous works, however we find more appropriate the term *lattice source*. We maintain the basic assumption that the data is generated as a convex combination of a set of lattice sources which are the vertices of a convex polytope covering some region of the input data. This assumption is similar to the linear mixture assumed by the ICA approach, however we do not impose any probabilistic assumption on the data. The lattice sources discovered by the ILSIA are equivalent to the GLM design matrix columns, and the

unmixing process is identical to the conventional least squares estimator. Therefore, LICA is a kind of unsupervised GLM whose regressor functions are mined from the input dataset. If we try to establish correspondences to the ICA, the lattice sources correspond to the unknown statistically independent sources and the mixing matrix is the one given by the abundance coefficients computed by least squares estimation.

The ILSIA is an improved formulation of the Endmember Induction Heuristic Algorithm proposed in [7]. Our approach to lattice source selection from the data is based on the conjecture equivalence between the Strong Lattice Independence and the Affine Independence [24]. The SLI needs two conditions: Lattice Independence and max/min dominance. Lattice Independence is detected based on results on fixed points for Lattice Autoassociative Memories (LAM) [22, 24, 29], and max/min dominance is tested using algorithms inspired in the ones described in [30]. An important improvement relative to previous attempts is the use of Chebyshev best approximation results [29] in order to reduce the number of selected vectors. The ILSIA is a greedy incremental algorithm that passes only once over the sample. It starts with a randomly picked input vector and tests each vector in the input dataset to add it to the set of lattice sources.

There are other methods [8, 24] based on LAM to obtain a set of SLI vectors. However these methods produce initially a large set of lattice sources that must be reduced somehow, either resorting to a priori knowledge or to selections based on Mutual Information or other similarity measures. In the ILSIA the candidate SLI vectors are discarded on the basis of the existence of a fixed point that gives a good approximation of it in the Chebyshev distance sense, which is a natural distance in this Lattice Computing setting.

The LICA approach falls in the field of Lattice Computing algorithms, which have been introduced in [7] as the class of algorithms that either apply lattice operators inf and sup or use lattice theory to produce generalizations or fusions of previous approaches. In [7] an extensive and updated list of references that can be labeled Lattice Computing can be found. This paper is an extension of the one presented at the LBM 2008 workshop inside the CLA 2008 conference [9].

The outline of the paper is as follows: Section 2 gives a brief recall of ICA. Section 3 introduces the linear mixing model. Section 4 presents a sketch of the theoretical relation between Lattice Independence and Linear (Affine) Independence through the LAM theory. Section 6 gives results on synthetic fMRI like data. Section 5 gives the definition of our Incremental Lattice Source Induction Algorithm (ILSIA). Section 7 presents results of the proposed approach on a case study. Section 8 provides some conclusions.

## 2. Independent Component Analysis (ICA)

The *Independent Component Analysis* (ICA) [13] assumes that the data is a linear combination of non Gaussian, mutually independent latent variables with an unknown mixing matrix. The ICA reveals the hidden independent sources and the mixing matrix. That is, given a set of observations represented by a $d$-dimensional vector $\mathbf{x}$, ICA assumes a generative model

$$\mathbf{x} = \mathbf{A}\mathbf{s}, \tag{1}$$

where $\mathbf{s}$ is the $M$ dimensional vector of independent sources and $\mathbf{A}$ is the $d \times M$ unknown basis matrix. The ICA searches for the linear transformation of the data $\mathbf{W}$, such that the projected variables

$$\mathbf{W}\mathbf{x} = \mathbf{s}, \tag{2}$$

are as independent as possible. It has been shown that the model is completely identifiable if the sources are statistically independent and at least $M - 1$ of them are non Gaussian. If the sources are gaussian the ICA transformation could be estimated up to an orthogonal transformation. Estimation of mixing and unmixing matrices can be done maximizing diverse objective functions, among them the non gaussianity of the sources and the likelihood of the sample.

We have used the FastICA [14] algorithm implementation available at [26]. We have also used the implementations of Maximum Likelihood ICA [11] (ML-ICA) which is equivalent to Infomax ICA, Mean Field ICA [12] (MF-ICA), and Molgedey and Schouster ICA (MS-ICA) based on dynamic decorrelation [16], which are available at [27].

Application of ICA to fMRI has been reviewed by [3]. Reports on the research application of ICA to fMRI signals include the identification of signal types (task related and physiology related) and the analysis of multisubject fMRI data. The most common approach is the spatial ICA that looks for spatial disjoint regions corresponding to the identified signal types. It has been claimed that ICA has identified several physiological noise sources as well as other noise sources (motion, thermodynamics) identifying task related signals. Diverse ICA algorithms have been tested in the literature with inconclusive results. Among them, FastICA, the one that we will apply in the case study, did identify the task related signals consistently. Among the clinical applications, ICA has been used to study the brain activation due to pain in healthy individuals versus those with chronic pain [1], the discrimination of Alzheimer's patients from healthy controls [10], the classification of schizophrenia [4] and studies about the patterns of brain activation under alcohol intoxication [4].

## 3. The linear mixing model and the Lattice Independent Component Analysis

The linear mixing model can be expressed as follows:

$$\mathbf{x} = \sum_{i=1}^{M} a_i \mathbf{e}_i + \mathbf{w} = \mathbf{E}\mathbf{a} + \mathbf{w}, \tag{3}$$

where $\mathbf{x}$ is the $d$-dimensional pattern vector corresponding to the fMRI voxel time series vector, $\mathbf{E}$ is a $d \times M$ matrix whose columns are the $d$-dimensional vectors $\mathbf{e}_i, i = 1, .., M$, which are called endmembers when they are the vertices of a convex region covering the data, $\mathbf{a}$ is the $M$-dimensional vector of linear mixing coefficients, which correspond to fractional abundances in the convex case, and $\mathbf{w}$ is the $d$-dimensional additive observation noise vector. The linear mixing model is subjected to two constraints on the abundance coefficients when the data points fall into a simplex whose vertices are the endmembers, all abundance coefficients must be non-negative $a_i \geq 0, i = 1, .., M$ and normalized to unity summation $\sum_{i=1}^{M} a_i = 1$. Under this

circumstance, we expect that the vectors in $\mathbf{E}$ are affinely independent and that the convex region defined by them includes *all* the data points. We recall that a set of vectors $X = \{\mathbf{x}_1, \ldots, \mathbf{x}_k\}$ is said to be linearly independent if the unique solution to the equation $\sum_{i=1}^{k} a_i \mathbf{x}_i = \mathbf{0}$ is given by $a_i = 0$ for all $i \in \{1, \ldots, k\}$. A set $X$ is an affinely independent set if the solution to the simultaneous equations $\sum_{i=1}^{k} a_i \mathbf{x}_i = \mathbf{0}$ and $\sum_{i=1}^{k} a_i = \mathbf{0}$ is given by $a_i = 0$ for all $i \in \{1, \ldots, k\}$. Therefore, linear independence is a necessary condition for affine independence but not viceversa. The model in equation (3) is shared by other linear analysis approaches, such as the General Linear Model (GLM) [5] and the Independent Component Analysis (ICA) [13] which do not view $\mathbf{E}$ as a set of endmembers but as regressors or independent sources.

Once the enmembers have been determined the unmixing process is the computation of the matrix inversion that gives the coordinates of each data point relative to the convex region vertices. The simplest approach is the unconstrained least squared error (LSE) estimation given by:

$$\widehat{\mathbf{a}} = \left(\mathbf{E}^T \mathbf{E}\right)^{-1} \mathbf{E}^T \mathbf{x}. \tag{4}$$

Even when the vectors in $\mathbf{E}$ are affine independent, the coefficients that result from equation (4) do not necessarily fulfill the non-negativity and unity normalization. Ensuring both conditions is a difficult computational problem. Some authors (i.e. [24]) use Non Negative Least Squares algorithms [15] to ensure at least non-negative coefficients. However in our works we use these mixture coefficients in a more qualitative way and we do not feel the need to enforce these conditions. Moreover, although the heuristic algorithm described in section 5 always produces the vertices of convex regions, these simplices always lie inside the data cloud, so that enforcing the non-negative and normalization conditions on the linear mixing coefficients would be impossible for some sample data points. Negative values are considered as zero values, for interpretation and visualization purposes, and the additivity to one condition is not important as long as we are looking for the maximum abundances to assign meaning to the resulting spatial distribution of the coefficients. These coefficients are interpreted as the regressor coefficients corresponding to the decomposition of the fMRI voxel time series into a basis of vectors. That is, high positive values are interpreted as high positive correlation with the time pattern of the corresponding lattice source. Therefore, to avoid confusion with the orthodox meaning of endmember, we will call *lattice source* to the set of affine independent vectors found by our algorithm.

We call *Lattice Independent Component Analysis* (LICA) the approach grounded in the results and algorithm that will be described in the following sections. LICA consists of two steps:

1. Induce from the given data a set of Strongly Lattice Independent vectors. In this paper we apply the Incremental Lattice Source Induction Algorithm (ILSIA) described in section 5. These vectors are taken as a set of affine independent vectors. The advantages of this approach are (1) that we are not imposing statistical assumptions, (2) that the algorithm is one-pass and very fast because it only uses comparisons and addition, (3) that it is unsupervised and incremental, and (4) that it detects naturally the number of lattice sources.
2. Apply the unconstrained least squares estimation to obtain the mixing matrix. The detection results are based on the analysis of the coefficients of this matrix.

Therefore, the approach is a combination of Linear and Lattice Computing: a linear component analysis where the components have been discovered by non-linear algorithms based on Lattice Theory.

## 4. Theoretical background on Lattice Independence and Lattice Autoassociative Memories

The work on Lattice Associative Memories (LAM) stems from the consideration of the bounded lattice ordered group (blog) $(\mathbb{R}_{\pm\infty}, \vee, \wedge, +, +')$ as the alternative to the computational framework given by the mathematical field $(\mathbb{R}, +, \cdot)$ for the definition of Neural Network algorithms. There $\mathbb{R}$ denotes the set of real numbers, $\mathbb{R}_{\pm\infty}$ the extended real numbers, $\wedge$ and $\vee$ denote, respectively, the binary $\max$ and $\min$ operations, and $+$, $+'$ denote addition and its dual operation. In our current context addition is self-dual. If $x \in \mathbb{R}_{\pm\infty}$, then its additive conjugate is $x^* = -x$. For a matrix $A \in \mathbb{R}_{\pm\infty}^{n\times m}$ its conjugate matrix is given by $A^* \in \mathbb{R}_{\pm\infty}^{n\times m}$, where each entry $a_{ij}^* = [A^*]_{ij}$ is given by $a_{ij}^* = (a_{ji})^*$.

The LAM were first introduced in [21, 20] as Morphological Associative Memories, a name still used in recent publications [29], but we follow the new convention introduced in [22, 24] because it sets the works in the more general framework of Lattice Computing. Given a set of input/output pairs of pattern $(X, Y) = \left\{\left(\mathbf{x}^\xi, \mathbf{y}^\xi\right); \xi = 1, .., k\right\}$, a linear heteroassociative neural network based on the pattern's cross correlation is built up as $W = \sum_\xi \mathbf{y}^\xi \cdot \left(\mathbf{x}^\xi\right)'$. Mimicking this constructive procedure [21, 20] propose the following constructions of Lattice Heteroassociative Memories (LHAM):

$$W_{XY} = \bigwedge_{\xi=1}^{k} \left[\mathbf{y}^\xi \times \left(-\mathbf{x}^\xi\right)'\right] \text{ and } M_{XY} = \bigvee_{\xi=1}^{k} \left[\mathbf{y}^\xi \times \left(-\mathbf{x}^\xi\right)'\right], \tag{5}$$

where $\times$ is any of the $\boxtimes$ or $\boxtimes$ operators. Here $\boxtimes$ and $\boxtimes$ denote the $\max$ and $\min$ matrix product [21, 20]. respectively defined as follows:

$$C = A \boxtimes B = [c_{ij}] \Leftrightarrow c_{ij} = \bigvee_{k=1,\ldots,n} \{a_{ik} + b_{kj}\}, \tag{6}$$

$$C = A \boxtimes B = [c_{ij}] \Leftrightarrow c_{ij} = \bigwedge_{k=1,\ldots,n} \{a_{ik} + b_{kj}\}. \tag{7}$$

If $X = Y$ then the LHAM memories are Lattice Autoassociative Memories (LAAM). Conditions of perfect recall by the LHAM and LAAM of the stored patterns proved in [21, 20] encouraged the research on them, because in the continuous case, the LAAM is able to store and recall any set of patterns: $W_{XX} \boxtimes X = X = M_{XX} \boxtimes X$, for any $X$. However, this result holds when we deal with noise-free patterns. Research on robust recall [19, 23, 20] based on the so-called kernel patterns lead to the notion of morphological independence, in the erosive and dilative sense, and finally to the definition of Lattice Independence (LI) and Strong Lattice Independence (SLI). We gather theoretical results from [22, 24, 29, 30] that set the theoretical background for the approach to lattice source induction described in section 5.

**Definition** Given a set of vectors $X = \left\{\mathbf{x}^1, ..., \mathbf{x}^k\right\} \subset \mathbb{R}^n$ a *linear minimax combination* of vectors from this set is any vector $\mathbf{x} \in \mathbb{R}^n_{\pm\infty}$ which is a *linear minimax sum* of these vectors:

$$x = \mathcal{L}\left(\mathbf{x}^1, ..., \mathbf{x}^k\right) = \bigvee_{j \in J} \bigwedge_{\xi=1}^{k} \left(a_{\xi j} + \mathbf{x}^\xi\right),$$

where $J$ is a finite set of indices and $a_{\xi j} \in \mathbb{R}_{\pm\infty}$ $\forall j \in J$ and $\forall \xi = 1, ..., k$.

**Definition** The *linear minimax span* of vectors $\left\{\mathbf{x}^1, ..., \mathbf{x}^k\right\} = X \subset \mathbb{R}^n$ is the set of all linear minimax sums of subsets of $X$, denoted $LMS\left(\mathbf{x}^1, ..., \mathbf{x}^k\right)$.

**Definition** Given a set of vectors $X = \left\{\mathbf{x}^1, ..., \mathbf{x}^k\right\} \subset \mathbb{R}^n$, a vector $\mathbf{x} \in \mathbb{R}^n_{\pm\infty}$ is *lattice dependent* if and only if $x \in LMS\left(\mathbf{x}^1, ..., \mathbf{x}^k\right)$. The vector $\mathbf{x}$ is *lattice independent* if and only if it is not lattice dependent on $X$. The set $X$ is said to be *lattice independent* if and only if $\forall \lambda \in \{1, ..., k\}$, $\mathbf{x}^\lambda$ is lattice independent of $X \setminus \left\{\mathbf{x}^\lambda\right\} = \left\{\mathbf{x}^\xi \in X : \xi \neq \lambda\right\}$.

The definition of lattice independence supersedes and improves the early definitions [23] of erosive and dilative morphological independence. This definition of lattice dependence is closely tied to the study of the fixed points of the LAAM's taken as operators.

**Theorem 4.1.** *[22, 29] Given a set of vectors $X = \left\{\mathbf{x}^1, ..., \mathbf{x}^k\right\} \subset \mathbb{R}^n$, a vector $\mathbf{y} \in \mathbb{R}^n_{\pm\infty}$ is a fixed point of $W_{XX}$, that is $W_{XX} \boxtimes \mathbf{y} = \mathbf{y}$, if and only if $\mathbf{y}$ is lattice dependent on $X$.*

**Definition** A set of vectors $X = \left\{\mathbf{x}^1, ..., \mathbf{x}^k\right\} \subset \mathbb{R}^n$ is said to be *max dominant* if and only if for every $\lambda \in \{1, ..., k\}$ there exists and index $j_\lambda \in \{1, ..., n\}$ such that

$$x^\lambda_{j_\lambda} - x^\lambda_i = \bigvee_{\xi=1}^{k} \left(x^\xi_{j_\lambda} - x^\xi_i\right) \forall i \in \{1, ..., n\}.$$

Similarly, $X$ is said to be *min dominant* if and only if for every $\lambda \in \{1, ..., k\}$ there exists and index $j_\lambda \in \{1, ..., n\}$ such that

$$x^\lambda_{j_\lambda} - x^\lambda_i = \bigwedge_{\xi=1}^{k} \left(x^\xi_{j_\lambda} - x^\xi_i\right) \forall i \in \{1, ..., n\}.$$

The expressions that compound this definition appeared in the early theorems about perfect recall of Morphological Associative Memories [21, 20]. Their value as an identifiable property of the data has been discovered in the context of the formalization of the relationship between strong lattice independence, defined below, and the affine independence in the classical linear analysis.

**Definition** A set of lattice independent vectors $\left\{\mathbf{x}^1, ..., \mathbf{x}^k\right\} \subset \mathbb{R}^n$ is said to be *strongly lattice independent* (SLI) if and only if $X$ is max dominant or min dominant or both.

As said before, min and max dominance are the conditions for perfect recall. Per construction, the column vectors of Lattice Autoassociative Memories are diagonally min or max dominant, depending of their erosive or dilative nature, therefore they will be strong lattice independent, *if* they are lattice independent.

**Conjecture 4.2.** *[24] If* $X = \left\{\mathbf{x}^1, ..., \mathbf{x}^k\right\} \subset \mathbb{R}^n$ *is strongly lattice independent then* $X$ *is affinely independent.*

This conjecture (stated as theorem in [22]) is the key result whose proof would relate the linear convex analysis and the non-linear lattice analysis. If true, it means that the construction of the LAAM provides the starting point for obtaining sets of affine independent vectors that could be used as lattice sources for the unmixing algorithms described in section 3. We have found it to be true in our computational experiences, but a formal proof is still lacking.

**Theorem 4.3.** *[24] Let* $X = \left\{\mathbf{x}^1, ..., \mathbf{x}^k\right\} \subset \mathbb{R}^n$ *and let* $W$ *(* $M$*) be the set of vectors consisting of the columns of the matrix* $W_{XX}$ *(*$M_{XX}$*). Let* $F(X)$ *denote the set of fixed points of the LAAM constructed from set* $X$*. There exist* $V \subset W$ *and* $N \subset M$ *such that* $V$ *and* $N$ *are strongly lattice independent and* $F(X) = F(V) = F(N)$ *or, equivalently,* $W_{XX} = W_{VV}$ *and* $M_{XX} = M_{NN}$*.*

The key idea of this theorem is that it is possible to built a set of SLI vectors from the column vectors of a LAAM. Taking into account that the column vectors of a LAAM are diagonally max or min dominant (depending on the kind of LAAM), it suffices to find a subset which is lattice independent. It is also grounded in the fact that a subset of a set of max or min dominant vectors is also min or max dominant. The proof of the theorem is constructive giving way to algorithms to find these sets of SLI. It removes iteratively the detected lattice dependent column vectors. Detection lies in the fact that $W_{XX} = W_{WW} = W_{VV}$ and $M_{XX} = M_{MM} = M_{NN}$ when the vectors removed from $W$ or $M$ to obtain $V$ or $N$ are lattice dependent on the remaining ones. Algorithms discussed in [8, 24] apply this result. The experience shows that most of the column vectors of the LAAM are lattice independent, so that the sets of SLI vectors are large and need some kind of selection algorithm to find the salient ones. One way to perform this selection is discarding those that can be interpreted as close approximations of others already selected, in the incremental framework of the algorithm described in section 5.

To deal with approximation in this Lattice Computing setting it seems natural [29] to use the Chebyshev distance given by the greatest componentwise absolute difference between two vectors, it is denoted $\varsigma(\mathbf{x}, \mathbf{y})$ and can be computed as follows: $\varsigma(\mathbf{x}, \mathbf{y}) = (\mathbf{x}^* \boxtimes \mathbf{y}) \vee (\mathbf{y}^* \boxtimes \mathbf{x})$. The Chebyshev-best approximation of $\mathbf{c}$ by $f(\mathbf{x})$ subject to $\mathbf{x} \in S$, is the minimization of $\varsigma(f(\mathbf{x}), \mathbf{c})$ subject to $\mathbf{x} \in S$.

**Theorem 4.4.** *[29] Given* $B \in \mathbb{R}^{m \times n}$ *and* $\mathbf{c} \in \mathbb{R}^m$*, a Chebyshev-best solution to the approximation of* $\mathbf{c}$ *by* $B \boxtimes \mathbf{x}$ *subject to the constraint* $B \boxtimes \mathbf{x} < \mathbf{c}$ *is given by* $\mathbf{x}^{\#} = B^* \boxtimes \mathbf{c}$ *and* $\mathbf{x}^{\#}$ *is the greatest such solution.*

In our incremental algorithm we will need to solve the unconstrained minimization problem

$$\min \varsigma \left( B \boxtimes \mathbf{x}, \mathbf{c} \right),$$

in order to decide if the input vector is already well approximated by a fixed point of the LAAM constructed from the selected enmembers.

**Theorem 4.5.** *[29]Given $B \in \mathbb{R}^{m \times n}$ and $\mathbf{c} \in \mathbb{R}^m$, a Chebyshev-best solution to the approximation of $\mathbf{c}$ by $B \boxtimes \mathbf{x}$ is given by $\mu + \mathbf{x}^{\#}$ where $\mu$ is such that $2\mu = \varsigma \left( B \boxtimes \mathbf{x}^{\#}, \mathbf{c} \right) = \left( B \boxtimes \mathbf{x}^{\#} \right)^{*} \boxtimes \mathbf{c}$.*

This theorem has resulted in enhanced robust recall for LAAM under general noise conditions, compared with other Associative Memories proposed in the literature. It has also been applied to produce a lattice based nearest neighbor classification scheme with good results on standard benchmark classification problems.

## 5. Incremental Lattice Source Induction Algorithm (ILSIA)

The algorithm described in this section is a further step in the formulation of a search of SLI sets of vectors from the Endmember Induction Heuristic Algorithm introduced in [8]. It is grounded in the formal results on continuous LAAM reviewed in the previous section. The dataset is denoted by $Y = \{\mathbf{y}_j; j = 1, \ldots, N\} \in \mathbb{R}^{n \times N}$ and the set of lattice sources induced from the data at any step of the algorithm is denoted by $X = \{\mathbf{x}_j; j = 1, \ldots, K\} \in \mathbb{R}^{n \times K}$. The number of lattice sources $K$ will vary from the initial value $K = 1$ up to the number of lattice sources found by the algorithm, we will skip indexing the set of lattice sources with the iteration time counter. The algorithm makes only one pass over the sample as in [8]. The auxiliary variables $\mathbf{s}_1, \mathbf{s}_2, \mathbf{d} \in \mathbb{R}^n$ serve to count the times that a row has the maximum and minimum, and the component wise differences of the lattice source and input vectors. Borrowing Matlab notation, the expression $(\mathbf{d} == m_1)$ denotes a vector of 0 and 1, where 1 means that corresponding components are equal.

The algorithm aims to produce sets of SLI vectors extracted from the input dataset. Assuming the truth of conjecture 4.2 the resulting sets are affine independent, that is, they define convex polytopes that cover some (most of) the data points in the dataset. To ensure that the resulting set of vectors are SLI, we first ensure that they are lattice independent in step 3(a) of Algorithm 1 by the application of theorem 4.1: each new input vector is applied to the LAAM constructed with the already selected lattice sources. If the recall response evoked by the vector is perfect, then it is lattice dependent on the lattice sources, and can be discarded. If not, then the new input vector is a candidate lattice source. We test in step 3(c) the min and max dominance of the set of lattice sources enlarged with the new input vector. We need to test the whole enlarged lattice source set because min and max dominance are not preserved when adding a vector to a set of min/max dominant vectors. Note that this is contrary to the fact that subsets of min or max dominant sets of vectors are also min or max dominant [24]. Note also that to test lattice independence we need only to build $W_{XX}$ because the set of fixed points is the same for both kinds of LAAM, i.e. $F\left(W_{XX}\right) = F\left(M_{XX}\right)$. However, we need

**Algorithm 1** Incremental Lattice Source Induction Algorithm (ILSIA)

1. Initialize the set of lattice sources $X = \{\mathbf{x}_1\}$ with a randomly picked vector in the input dataset $Y$.
2. Construct the LAAM based on the strong lattice independent (SLI) vectors: $W_{XX}$.
3. For each data vector $\mathbf{y}_j$;j=1,. . .,N
   (a) if $\mathbf{y}_j = W_{XX} \boxtimes \mathbf{y}_j$ then $\mathbf{y}_j$ is lattice dependent on the set of lattice sources $X$, skip further processing.
   (b) if $\varsigma\left(W_{XX} \boxtimes \left(\mu + \mathbf{x}^{\#}\right), \mathbf{y}_j\right) < \theta$, where $\mathbf{x}^{\#} = W^{*}_{XX} \boxtimes \mathbf{y}_j$ and $\mu = \frac{1}{2}\left(\left(W_{XX} \boxtimes \mathbf{x}^{\#}\right) \boxtimes \mathbf{y}_j\right)$, then skip further processing.
   (c) test max/min dominance to ensure SLI, consider the enlarged set of lattice sources $X' = X \cup \{\mathbf{y}_j\}$
      i. $\mu_1 = \mu_2 = 0$
      ii. for $i = 1, \ldots, K+1$
      iii. $\mathbf{s}_1 = \mathbf{s}_2 = \mathbf{0}$
         A. for $j = 1, \ldots, K+1$ and $j \neq i$
            $\mathbf{d} = \boldsymbol{x}_i - \mathbf{x}_j$; $m_1 = \max(\mathbf{d})$; $m_2 = \min(\mathbf{d})$.
            $\mathbf{s}_1 = \mathbf{s}_1 + (\mathbf{d} == m_1)$, $\mathbf{s}_2 = \mathbf{s}_2 + (\mathbf{d} == m_2)$.
         B. $\mu_1 = \mu_1 + (\max(\mathbf{s}_1) == K)$ or $\mu_2 = \mu_2 + (\max(\mathbf{s}_2) == K)$.
      iv. If $\mu_1 = K+1$ or $\mu_1 = K+1$ then $X' = X \cup \{\mathbf{y}_j\}$ is SLI, go to 2 with the enlarged set of lattice sources and resume exploration from $j+1$.
4. The final set of lattice sources is $X$.

to test both min and max dominance because SLI needs one of them or both to hold. This part of the algorithm is an adaptation of the procedure proposed in [30].

If SLI was the only criteria to be tested to include input vectors in the set of lattice sources, then we will end up detecting a large number of lattice sources so that there will be little significance of the abundance coefficients because many of them will be closely placed in the input vector space. This is in fact the main inconvenient of the algorithms proposed in [8, 24] that use the columns of a LAAM constructed from the data as the SLI vector set, after removing lattice dependent vectors. To reduce the set of lattice sources selected we apply the results on Chebyshev-best approximation in theorem 4.5 discarding input vectors that can be well approximated by a fixed point of the LAAM constructed from the current set of lattice sources. In step 3(b) this approximation of a candidate is tested before testing max/min dominance: if the Chebyshev distance from the best approximation to the input vector is below a given threshold, the input vector is considered a noisy version of a vector which is lattice dependent on the current set of lattice sources.

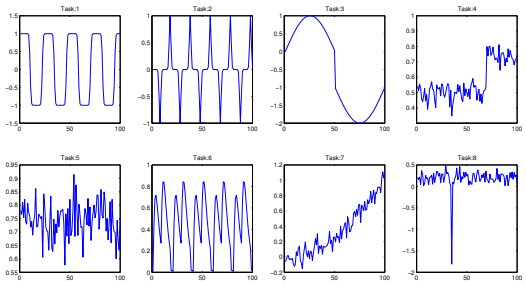


Figure 1: Simulated sources (time courses) in the experimental data.

## 6. Results on simulated fMRI images

We have used the simulated fMRI data [2, 31] [1]. In fMRI the spatial distribution of data sources can be classified into locations of interest and artifacts. The locations of interest include task-related, transiently task-related, and function-related locations. Their spatial distribution are typically super-gaussian in nature because of the high localization of brain functionality. A task-related location and its corresponding source (component) closely match the experimental paradigm. A transiently task-related source, on the other hand, is similar to a task-related source but with an activation that may be pronounced during the beginning of each task cycle and may fade out or change as time progresses. Functional locations are those activated areas which are related to a particular functional area of the brain and the source for these may not exhibit a particular pattern. The class of uninteresting sources or artifacts include motion related sources due to head movement, respiration, and cardiac pulsation. Figure 1 shows the sources used in the simulated fMRI data. Source #1 corresponds to the task related time course, source #6 corresponds to a transient task-related time course. Figure 2 shows the spatial distribution of the locations of the sources, corresponding to the mixing matrices in the linear models of both ICA and LICA. Spatial locations #1 and #6 are the ones with most interest from the task point of view. To form the fMRI mixture, first the image data is reshaped into vectors by concatenating columns of the image matrix. The source matrix is multiplied by the time course matrix to obtain a mixture that simulates 100 scans of a single slice of fMRI data.

We have applied the LICA and MS-ICA algorithms to this simulated data. We obtain five lattice sources with the LICA approach using standard settings of the algorithm, and we set the MS-ICA number of sources to that number. Figure 3 presents the lattice sources found by ILSIA, with the best correlated simulated time course overlaid in red. Figure 4 shows the sources found by the MS-ICA together with the best correlated simulated time course. Note that ILSIA finds both a task related and a function-related source. We show in figure 5 the abundance images that correspond to the spatial

[1] Simulated data can be generated with the tools provided in http://mlsp.umbc.edu/simulated_fmri_data.html

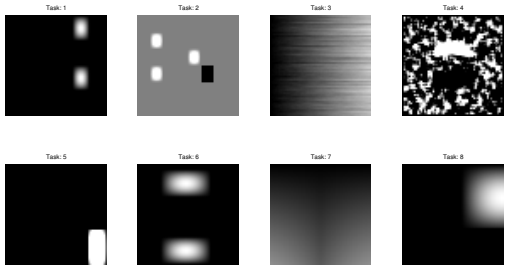


Figure 2: Simulated spatial distribution of location of the sources

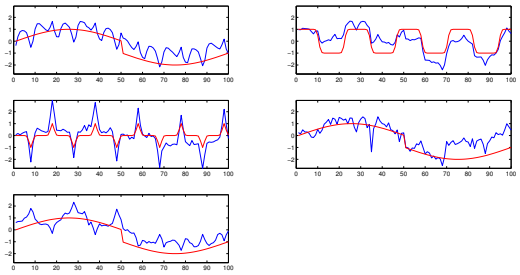

Figure 3: Sources found by the ILSIA on the simulated data

distributions of the lattice sources. Notice that the spatial location of the task-related source is well detected in the second image, while the transient task-related source location is also well detected despite that it does not appear as one of the best correlated sources in figure 14. Because the LICA and ICA algorithms are unsupervised, they can discover sources which indirectly help discover the spatial locations of interest, although the sources themselves are not precise matches of the underlying true sources. Figure 6 shows the spatial distribution of the MS-ICA sources. The detection is noisier than in the results obtained by LICA, and the task-related spatial locations are not so clearly detected. Table 1 contains the quantitative measure of the goodness of spatial discovery, given by the Mutual Information similarity measure between the simulated spatial distributions of the simulated sources and the mixing coefficients that give the estimation of the spatial distribution of the discovered sources. We have highlighted the maximum values per column, and we have highlighted the closest one when it is near the maximum of the column. The MS-ICA has more ambiguous columns than the LICA, which is in agreement with the visual assessment of figures 5 and 6.

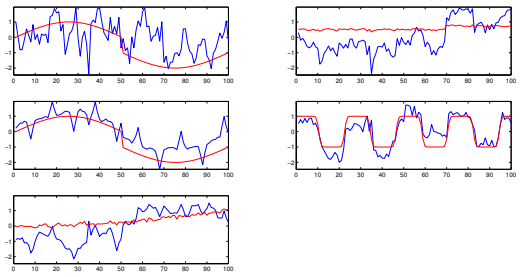

Figure 4: Sources found by MS-ICA on the simulated data

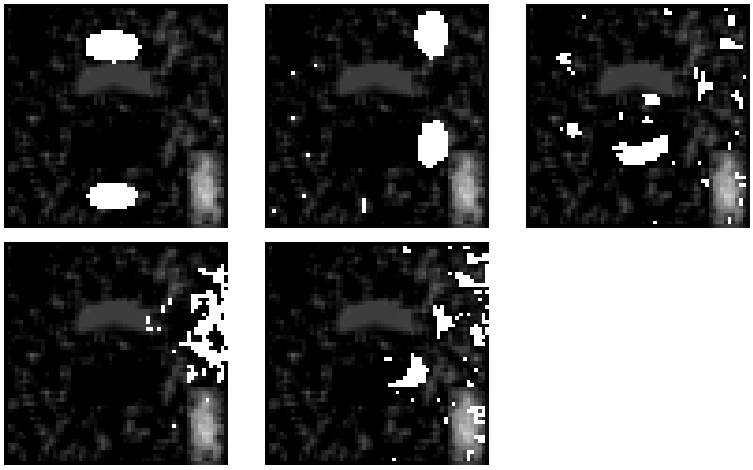

Figure 5: Spatial distributions found by LICA on the simulated data.

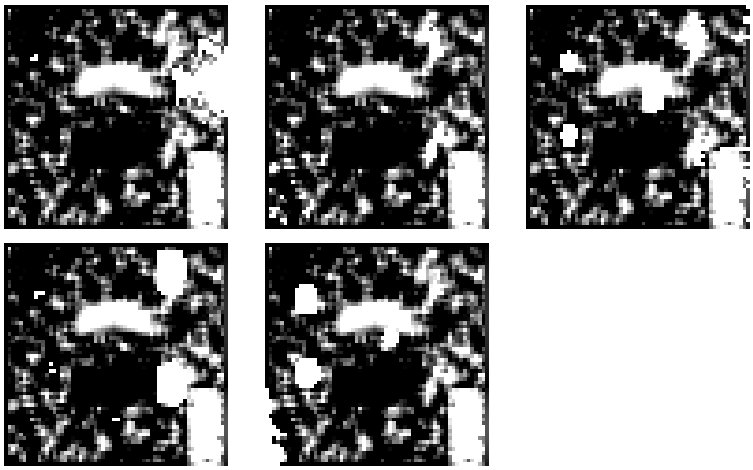

Figure 6: Spatial distribution of the sources given by the mixing matrices of MS-ICA on the simulated data.

| | MS-ICA | | | | | LICA | | | | |
|---|---|---|---|---|---|---|---|---|---|---|
| Source | #1 | #2 | #3 | #4 | #5 | #1 | #2 | #3 | #4 | #5 |
| #1 | -0,16 | 0,15 | 0,03 | **1,18** | -0,36 | -0,52 | **2,51** | -0,37 | -0,23 | 0,02 |
| #2 | -0,45 | -0,78 | -0,13 | -0,38 | -0,29 | -0,48 | -0,33 | **2,26** | -0,13 | -0,38 |
| #3 | **1,29** | **1,09** | **2,32** | **0,79** | **1,18** | 0,31 | 1,66 | 0,25 | **2,42** | **2,24** |
| #4 | -0,28 | 0,68 | -0,56 | -0,63 | -0,38 | -0,57 | -0,72 | -0,53 | -0,52 | -0,50 |
| #5 | -1,42 | -1,05 | -0,80 | -0,69 | -0,70 | -0,71 | -0,76 | -0,70 | -0,57 | -0,72 |
| #6 | **1,33** | -0,79 | -0,30 | -0,39 | -0,60 | **2,26** | -0,44 | 0,36 | -0,50 | -0,54 |
| #7 | 0,62 | **1,51** | 0,17 | -0,24 | **0,80** | 0,30 | -0,20 | -0,57 | -0,01 | 0,55 |
| #8 | -0,92 | -0,81 | -0,72 | -0,63 | -0,62 | -0,59 | -0,71 | -0,68 | -0,47 | -0,67 |

Table 1: Mutual Information similitude between the spatial locations discovered by LICA and MA-ICA and the ground truth spatial locations.

## 7. Results on a standard case study

The experimental data for this benchmarking corresponds to auditory stimulation test data of a single person[2]. These whole brain BOLD/EPI images were acquired on a modified 2T Siemens MAGNETOM Vision system. Each acquisition consisted of 64 contiguous slices. Each slice being a 2D image of one head volume cut. There are 64x64x64 voxels of size 3mm x 3mm x 3mm. The data acquisition took 6.05s., with the scan-to-scan repeat time (RT) set arbitrarily to 7s., 96 acquisitions were made (RT=7s.) in blocks of 6, i.e., 16 blocks of 42s. duration. The condition for successive blocks alternated between rest and auditory stimulation, starting with rest. Auditory stimulation was bi-syllabic words presented binaurally at a rate of 60 per minute. Due to T1 effects it is advisable to discard the first few scans (there were no "dummy" lead-in scans). We have discarded the first 10 scans. An standard results obtained with the SPM software is presented in figure 7 as localized in the Talairach space, in sagital, coronal and axial cuts.

There are a number of sources of noise in the fMRI signal [28] that must be dealt with in appropriate preprocessing steps [25]. We have dealt with these noise sources following the standard procedures in SPM software, so that all the algorithms applied have the same input data quality. First, we realigned the volumes to account for head motion artifacts. Second, we coregistered the functional volumes with the structural MRI T1-weighted volume. Third, we performed spatial normalization guided by the structural volume segmentation. Finally, we performed a smoothing step with an isotropic Gaussian kernel.

As already discussed in [9], we perform a Lattice Normalization, subtracting the mean value of each voxel time series independently so that the plots are collapsed around the origin. This mean subtraction corresponds to an scale normalization in the Lattice Computing sense. It removes scale effects that hinder the detection of meaningful lattice independent vectors. Note that, although we are shifting the voxel vector

[2]The dataset is freely available from ftp://ftp.fil.ion.ucI.ac.uk/spm/data, the file name is snrfM00223.zip. The functional data starts at acquisition 4, image snrfMOO223-004.

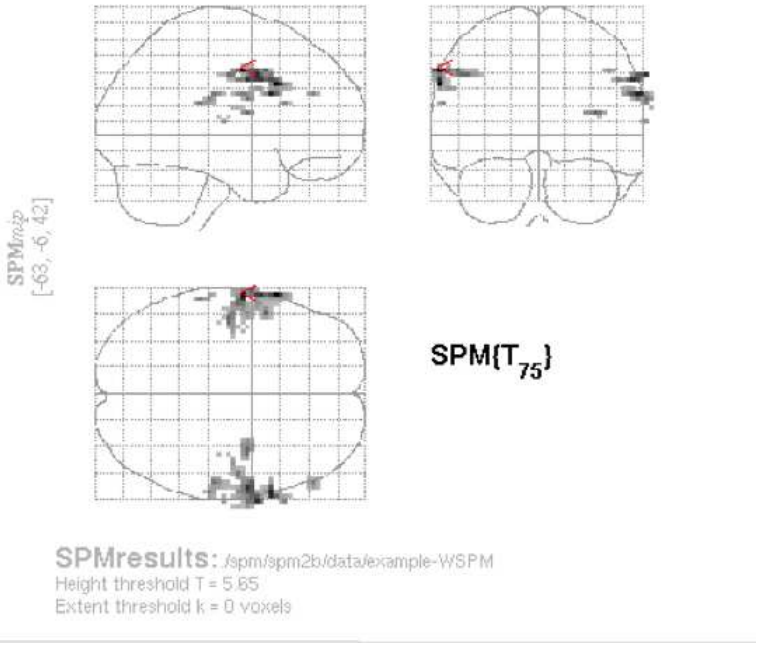


Figure 7: Activation maps obtained with an execution of SPM software with nominal parameters over the case study data.

| # | PCA | ML-ICA | MF-ICA | MS-ICA | FastICA | LICA |
|---|---|---|---|---|---|---|
| 1 | 0.04 | -0.14 | -0.13 | -0.04 | -0.06 | **0.20** |
| 2 | 0.02 | 0.09 | -0.14 | **0.22** | -0.16 | 0.09 |
| 3 | -0.08 | -0.01 | 0.12 | -0.07 | 0.08 | -0.07 |
| 4 | -0.22 | -0.03 | -0.13 | 0.07 | -0.12 | 0.17 |
| 5 | 0.03 | **0.37** | -0.13 | -0.20 | -0.18 | 0.14 |
| 6 | 0.10 | 0.12 | -0.12 | -0.13 | 0.11 | 0.09 |
| 7 | 0.33 | 0.12 | -0.04 | -0.07 | -0.10 | -0.15 |
| 8 | **0.34** | -0.09 | 0.05 | 0.19 | 0.03 | -0.07 |
| 9 | -0.15 | 0.18 | 0.11 | 0.06 | **0.25** | 0.06 |
| 10 | -0.09 | -0.14 | -0.18 | 0.16 | 0.05 | 0.02 |
| 11 | 0.24 | -0.15 | **0.15** | -0.25 | -0.07 | 0.09 |

Table 2: Correlation between lattice sources found by LICA, the sources found by the ICA algorithms, the PCA's eigenvectors and the task control variable.

to the origin, we are not aiming to perform a normalization in the statistical sense.

We have proceeded as follows: first we have applied the ILSIA algorithm, described in section 5, obtaining a number of lattice sources. Then we have applied the comparative algorithms (PCA, ML-ICA, MF-ICA, MS-ICA and FastICA) setting the number of lattice sources to the number obtained by LICA. Table 2 shows the correlation of the induced lattice sources and independent sources with the time plot of the experiment control variable, which is zero during the resting state and one while the auditory stimulation is taking place. This correlation is a measure of how well each lattice source/source is related to the task. The source with the maximum correlation for each algorithm is an indication of the a corresponding spatial distribution of mixing coefficients that may have the best similitude with the SPM activation results of figure 7. To verify this hypothesis, we further computed the Mutual Information similitude measure among the mixing coefficients of each source and the SPM t-statistics map before thresholding. Table 3 contains these Mutual Information values, which in general confirm the results of table 2. Therefore, we discover both the underlying task (which is set for the GLM in SPM) and the activation pattern. A qualitative assessment of the algorithms follows by visual comparison of the results of SPM (shown in figure 7) with the voxel clusters detected on the mixing coefficient volumes with highest Mutual Information for each algorithm. Cluster detection in the abundance images corresponds to voxels with abundance value above the 99% percentile of the distribution of this lattice source/source abundance coefficients over the whole volume. Cluster detection is shown as white voxels in the corresponding images. The goal is to reproduce the activity detection in the auditory cortex that the SPM is able to find. To asses this detection we reproduce selected axial, coronal and sagital cuts that correspond approximately to the brain cuts shown in the reference SPM result image shown in figure 7. In figures 8 to 13, the top row shows the axial and coronal cuts and the bottom row will show the sagital cuts lying approximately in the auditory cortex at both sides of the brain. Notice that in some cases there are activations detected over the air region, which an undesirable result.

| # | PCA | ML-ICA | MF-ICA | MS-ICA | FastICA | LICA |
|---|---|---|---|---|---|---|
| 1 | -0.30 | -0.21 | -0.17 | -0.37 | -0.97 | **3,02** |
| 2 | 0.02 | -045 | -0.46 | **1.48** | -1.60 | -0.30 |
| 3 | -0.30 | -0.71 | -0.46 | -1.17 | 0.34 | -0.30 |
| 4 | -0.22 | -0.85 | -0.43 | 0.53 | 1.11 | -0.30 |
| 5 | -0.03 | **2.60** | -0.46 | -0.39 | -0.76 | -0.30 |
| 6 | -0.30 | -0.56 | -0.46 | -0.98 | 0.18 | -0.30 |
| 7 | 0.33 | -0.78 | -0.46 | -0.13 | -0.59 | -0.30 |
| 8 | **3.020** | -0.09 | -0.38 | 1.35 | 0.30 | -0.30 |
| 9 | -0.35 | -0.52 | 0.02 | -1.29 | **1.99** | -0.30 |
| 10 | -0.39 | 0.75 | 0.35 | -0.21 | -0.30 | -0.30 |
| 11 | 0.24 | -0.06 | **2.91** | 1.17 | 0.31 | -0.30 |

Table 3: Mutual Information similarity between the mixing volumes computed by LICA, the ICA algorithms, the PCA and the t-statistic computed by the SPM software (before thresholding).

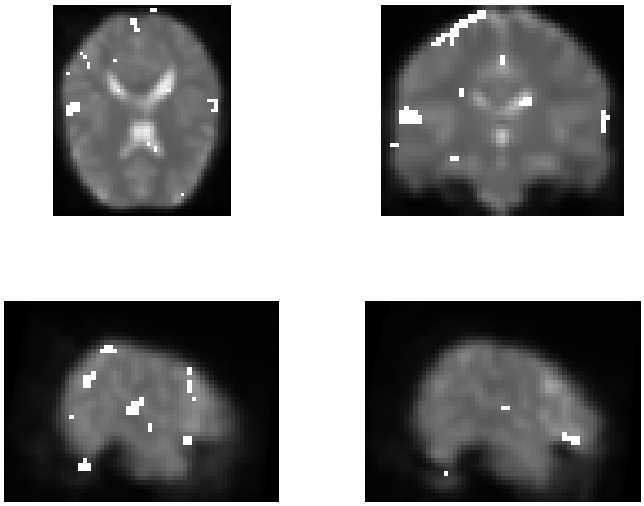

Figure 8: Best matching activation detection over the abundances of the LICA approach.

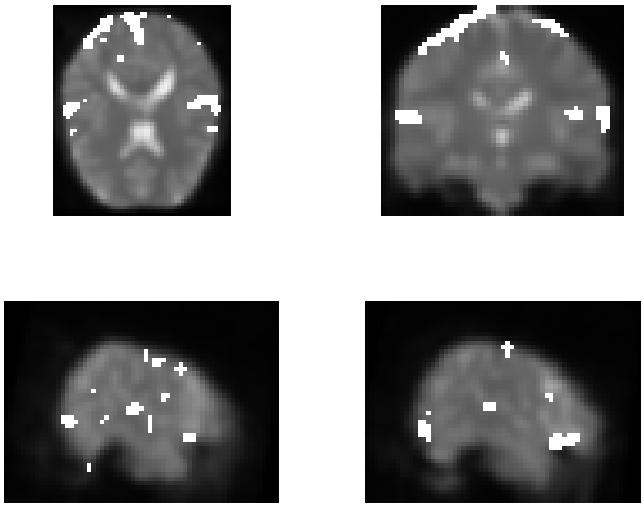

Figure 9: Best matching activation detection over the abundances of the PCA approach.

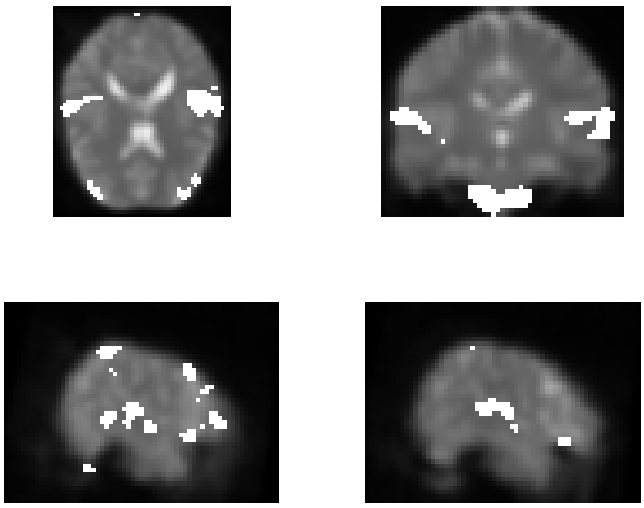

Figure 10: Best matching activation detection over the abundances of the ML-ICA approach.

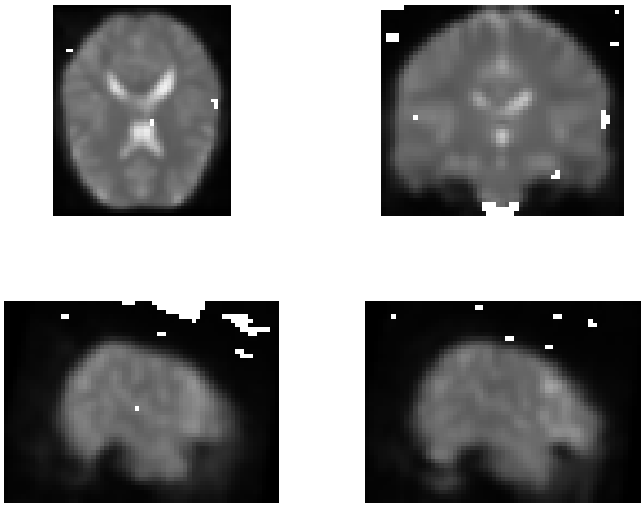

Figure 11: Best matching activation detection over the abundances of the MS-ICA approach.

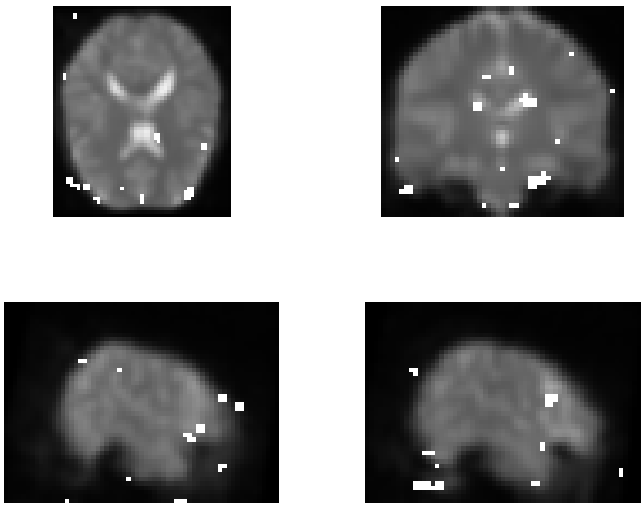

Figure 12: Best matching activation detection over the abundances of the FastICA approach.

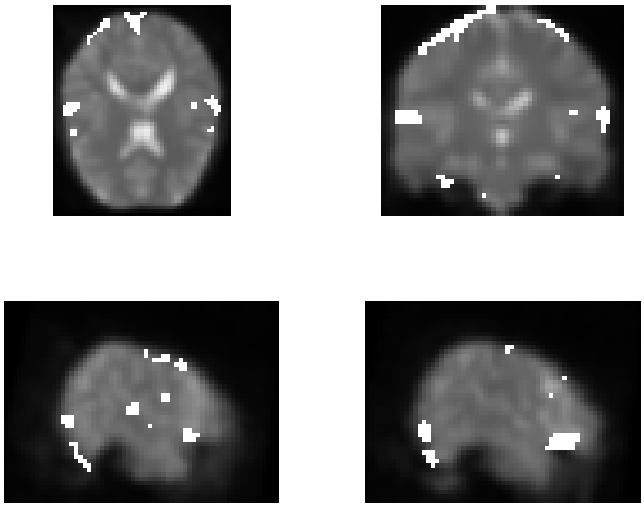

Figure 13: Best matching activation detection over the abundances of the MF-ICA approach.

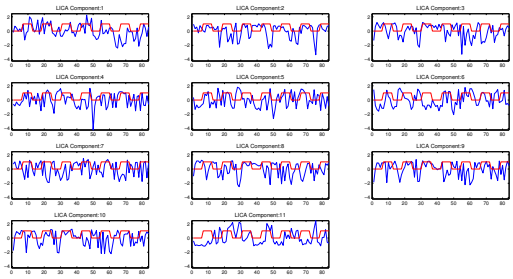


Figure 14: Lattice sources found by ILSIA, after normalization, for the LICA approach. Task indicator variable overlaid in red.

To show the degree of discovery of the control variable that models the control task by each algorithm, we reproduce in figures 14 to 19 the sources found by each algorithm, the lattice sources of LICA, the statistically independent sources of ICA, and the eigenvectors of the PCA. For this visualization, each source has been normalized computing its z-score, in order to highlight its structure and made it visually comparable with the control variable. The control variable plot is overlaid in read on each source plot.

We note that our approach gives qualitative and quantitative results comparable to the well established ICA approaches. That seems to support the idea that Lattice Independence involves properties somehow least similar to that of Statistical Independence.

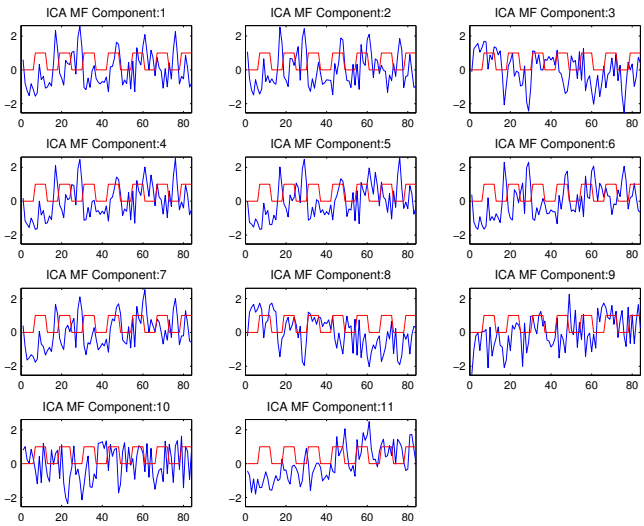


Figure 15: Sources found by MF-ICA, after normalization. Task indicator variable overlaid in red.

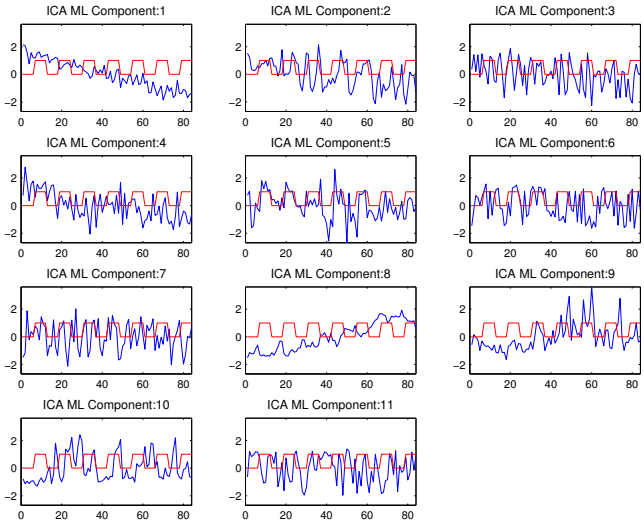


Figure 16: Sources found by ML-ICA, after normalization. Task indicator variable overlaid in red.

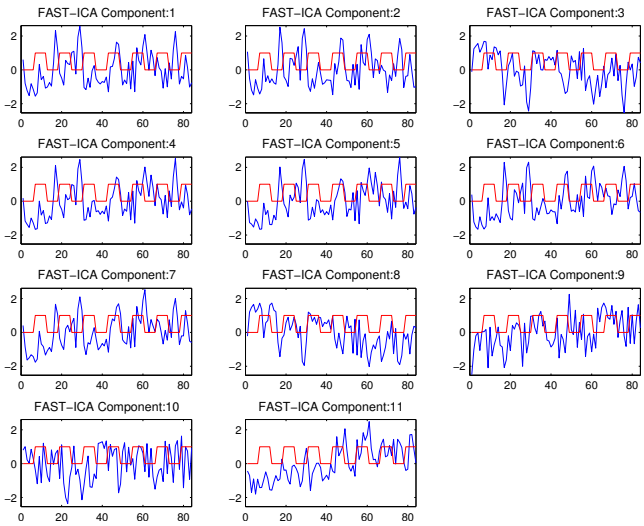


Figure 17: Sources found by FastICA, after normalization. Task indicator variable overlaid in red.

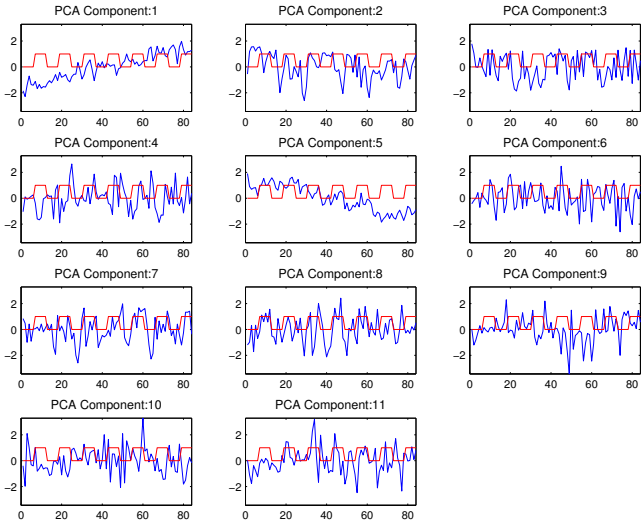


Figure 18: Eigenvectors found by PCA, after normalization. Task indicator variable overlaid in red.

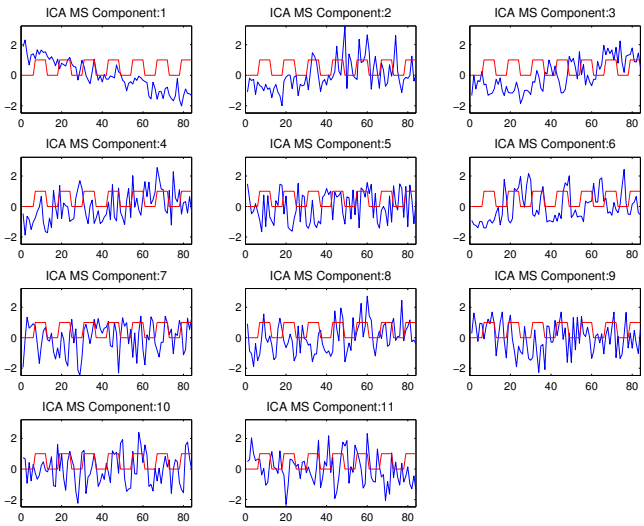


Figure 19: Sources found by MS-ICA, after normalization. Task indicator variable overlaid in red.

## 8. Summary and Conclusions

We have proposed and applied a Lattice Independent Component Analysis (LICA) to the model-free (unsupervised) analysis of fMRI. The LICA is based on the application of the Lattice Computing based algorithm ILSIA for the selection of the lattice sources, and the linear unmixing of the data based on these lattice sources. We have discussed the similarities of our approach with the application of ICA to fMRI activation detection [3, 25]. In our approach the temporal sources correspond to lattice sources detected by the ILSIA algorithm and the spatial mixing coefficients correspond to the abundance volumes obtained by unmixing the voxel time series on the basis of the found lattice sources. We have benefited from recent results on the Chebyshev best approximation and on the equivalence between SLI and affine independence. After a normalization consisting in the subtraction of the vector mean value, we look for SLI vectors that can not be well approximated by a fixed point of the LAAM constructed with the selected lattice sources. The LICA approach then uses this set of vectors to compute the mixing coefficients that characterize the data and the lattice source. We perform the activation detection thresholding these coefficients on the basis of its histogram. Work on simulated fMRI data shows that LICA performance is comparable to or improves over the ICA approach in the sense of discovering task-related sources and their spatial locations. Working with a well-known case study, have found that LICA gives results consistent with the SPM standard approach. Compared to ICA algorithms, LICA reproduces also the SPM results. An important feature of our approach is that it is an unsupervised algorithm, where we do not need to postulate *a priori* information or models. Also, LICA does not impose a probabilistic model on the sources. The lattice independence condition may be a more relaxed restriction to find meaningful sources in data where ICA approaches can fail due to their statistical properties.

Besides some other open theoretical questions, we want to state conveniently, and solve, the problem of finding the *right* number of lattice sources, and the *right* lattice sources. Those are non trivial problems in many other context (i.e. clustering), stated and solved as some kind of minimization problem. In our context, the problem is further complicated by the intrinsic non-linearity of ILSIA and the interleaving of the linear and non-linear procedures in LICA. It is not evident at this moment how to formulate a *well behaved* objective function for such purposes. Besides these fundamental problems, we will extend the validation evidence that may give the confidence to apply the method to new fMRI data sets as an exploratory tool by itself. We wishfully think that it could be applied to event oriented experiments, and to the task of discovering networks of activation in the brain.

**Acknowledgements**

We are grateful to the comments of the anonymous reviewers, which have helped us to improve the paper. The fruitful discussions with Dr. A. López de Munain and Dr. Sistiaga, from the Neurology Department, Donostia Hospital, which is embedded in the *Centro de Investigación Biomédica en Red sobre Enfermedades Neurodegenerativas* (CIBERNED) are also appreciated.

**References**

[1] A.L. Buffington, C.A. Hanlon, and M.J. McKeown. Acute and persistent pain modulation of attention-related anterior cingulate fmri activations. *Pain*, 113:172–184, 2005.

[2] V. Calhoun, G. Pearlson, and T. Adali. Independent component analysis applied to fMRI data: A generative model for validating results. *The Journal of VLSI Signal Processing*, 37(2):281–291, June 2004.

[3] V.D. Calhoun and T. Adali. Unmixing fMRI with independent component analysis. *Engineering in Medicine and Biology Magazine, IEEE*, 25(2):79–90, 2006.

[4] V.D. Calhoun, J.J. Pekar, and G.D. Pearlson. Alcohol intoxication effects on simulated driving: Exploring alcohol-dose effects on brain activation using functional mri. *Neuropsychopharmacology*, 29(11):2097–2107, 2004.

[5] K.J. Friston, J.T. Ashburner, S.J. Kiebel, T.E. Nichols, and Penny W.D. (eds.). *Statistical Parametric Mapping, the analysis of functional brain images*. Academic Press, 2007.

[6] K.J. Friston, A.P. Holmes, K.J. Worsley, J.P. Poline, C.D. Frith, and R.S.J. Frackowiak. Statistical parametric maps in functional imaging: A general linear approach. *Hum. Brain Map.*, 2(4):189–210, 1995.

[7] M. Graña. A brief review of lattice computing. In *Proc. WCCI 2008*, pages 1777–1781, 2008.

[8] M. Graña, I. Villaverde, J.O. Maldonado, and C. Hernandez. Two lattice computing approaches for the unsupervised segmentation of hyperspectral images. *Neurocomputing*, 72(10-12):2111–2120, 2009.

[9] Manuel Graña, M. García-Sebastian, I. Villaverde, and E. Fernández. An approach from lattice computing to fMRI analysis. In *LBM 2008 (CLA 2008), Proceedings of the Lattice-Based Modeling Workshop*, pages 33–44, 2008.

[10] M.D. Greicius, G. Srivastava, A.L. Reiss, and V. Menon. Default-mode network activity distinguishes alzheimer's disease from healthy aging: Evidence from func- tional mri. *Proc. Nat. Acad. Sci. U.S.A.*, 101(13):4637–4642, 2004.

[11] L. K. Hansen, J. Larsen, and T. Kolenda. Blind detection of independent dynamic components. *In proc. IEEE ICASSP'2001*, 5:3197–3200, 2001.

[12] P. Højen-Sørensen, O. Winther, and L.K. Hansen. Mean field approaches to independent component analysis. *Neural Computation*, 14:889–918, 2002.

[13] A. Hyvärinen, J. Karhunen, and E. Oja. *Independent Component Analysis*. John Wiley & Sons, New York, 2001.

[14] A. Hyvärinen and E. Oja. A fast fixed-point algorithm for independent component analysis. *Neural Comp.*, 9:1483–1492, 1997.

[15] C.L. Lawson and H.J. Hanson. *Solving least squares problems*. Prentice-Hall, (1974) Englewoods Cliffs NJ, 1974.

[16] L. Molgedey and H. Schuster. Separation of independent signals using time-delayed correlations. *Physical Review Letters*, 72(23):3634–3637, 1994.

[17] H.-P. Muller, E. Kraft, A. Ludolph, and S.N. Erne. New methods in fMRI analysis. *Engineering in Medicine and Biology Magazine, IEEE*, 21(5):134–142, 2002.

[18] J.J. Pekar. A brief introduction to functional MRI. *Engineering in Medicine and Biology Magazine, IEEE*, 25(2):24–26, 2006.

[19] B. Raducanu, M. Graña, and X. Albizuri. Morphological scale spaces and associative morphological memories: results on robustness and practical applications. *J. Math. Imaging and Vision*, 19(2):113–122, 2003.

[20] G. X. Ritter, J. L. Diaz-de Leon, and P. Sussner. Morphological bidirectional associative memories. *Neural Networks*, 12:851–867, 1999.

[21] G. X. Ritter, P. Sussner, and J. L. Diaz-de Leon. Morphological associative memories. *IEEE Trans. on Neural Networks*, 9(2):281–292, 1998.

[22] G.X. Ritter and P. Gader. Fixed points of lattice transforms and lattice associative memories. In P. Hawkes, editor, *Advances in Imaging and Electron Physics*, volume 144, pages 165–242. Elsevier, San Diego, CA., 2006.

[23] G.X. Ritter, G. Urcid, and L. Iancu. Reconstruction of patterns from noisy inputs using morphological associative memories. *J. Math. Imaging and Vision*, 19(2):95–112, 2003.

[24] G.X. Ritter, G. Urcid, and M.S. Schmalz. Autonomous single-pass endmember approximation using lattice auto-associative memories. *Neurocomputing*, 72(10-12):2101–2110, 2009.

[25] G.E. Sarty. *Computing Brain Activation Maps from fMRI Time-Series Images*. Cambridge University Press, 2007.

[26] FastICA site. http://www.cis.hut.fi/projects/ica/fastica/.

[27] ICA site. http://isp.imm.dtu.dk/toolbox/ica/index.html.

[28] S.C. Strother. Evaluating fMRI preprocessing pipelines. *Engineering in Medicine and Biology Magazine, IEEE*, 25(2):27–41, 2006.

[29] P. Sussner and M.E. Valle. Gray-scale morphological associative memories. *IEEE trans. Neural Networks*, 17(3):559–570, 2006.

[30] G. Urcid and J.C. Valdiviezo. Generation of lattice independent vector sets for pattern recognition applications. In *Mathematics of Data/Image Pattern Recognition, Compression, Coding, and Encryption X with Applications*, volume 6700, pages 1–12. Proc of SPIE, 2007.

[31] W Xiong, Y-O Li, H. Li, T. Adali, and V. D Calhoun. On ICA of complex-valued fMRI: advantages and order selection. In *Acoustics, Speech and Signal Processing, 2008. ICASSP 2008. IEEE International Conference on*, pages 529 –532, April 2008.